

Onset of topological quantum chaos in strongly correlated electron systems

V. A. Khodel,^{1,2} J. W. Clark,^{2,3} and M. V. Zverev^{1,4}

¹*National Research Centre Kurchatov Institute, Moscow, 123182, Russia*

²*McDonnell Center for the Space Sciences & Department of Physics,
Washington University, St. Louis, MO 63130, USA*

³*Centro de Investigação em Matemática e Aplicações,*

University of Madeira, 9020-105 Funchal, Madeira, Portugal

⁴*Moscow Institute of Physics and Technology, Dolgoprudny, Moscow District 141700, Russia*

We address manifestations of quantum chaos at temperatures T far below the Debye temperature T_D associated with the onset of classical behavior, effects that are well documented in experimental studies of strongly correlated electron systems. We attribute this unexpected phenomenon to spontaneous rearrangement of the conventional Landau state beyond a critical point at which the *topological* stability of this state breaks down, leading to the formation of an interaction-induced flat band adjacent to the nominal Fermi surface. We demonstrate that beyond the critical point, the quasiparticle picture of such correlated Fermi systems still holds, since the damping of single-particle excitations remains small compared with the Fermi energy $T_F = p_F^2/2m_e$. A Pitaevskii-style equation for determination of the new quasiparticle momentum distribution $n_*(\mathbf{p})$ is derived, which provides for explanation of the linear-in- T behavior of the resistivity $\rho(T)$ found experimentally. The interplay between this scenario for non-Fermi-liquid behavior of $\rho(T)$ and an alternative picture based on the notion of Planckian dissipation is discussed.

Currently, “topological” has become one of the most commonly used terms in condensed-matter physics, surpassing “quantum critical point.” It is sufficient to mention such collocations as topological order, topological transition, and topological insulator. In this report, we address manifestations of a *topological quantum chaos* related to radical alteration of customary cold-quantum-matter properties, which traditionally involve a relatively small fraction of single-particle degrees of freedom associated with the existence of a Fermi surface.

Quantum chaos, quantitatively and behaviorally attributed herein to the presence of a finite entropy excess S_* at temperatures $T \ll T_D$ has generally not been envisioned as a playmaker in modern low-temperature condensed-matter physics, since it is seemingly inconsistent with the Nernst theorem requiring $S(T)$ to vanish upon reaching $T = 0$. However, recent developments warrant a revision of this conventional stance. The first symptoms appeared in measurements [1, 2] of the thermal expansion coefficient $\alpha(T) = -V^{-1}\partial V/\partial T = V^{-1}\partial S/\partial P$ of the strongly correlated heavy-fermion superconductor CeCoIn₅, which has a tiny critical value $T_c = 2.3$ K at which superconductivity terminates. Although experimental results are indeed consistent with obedience of the Nernst theorem requiring $\alpha(0) = 0$, it is nevertheless of paramount significance that at extremely low temperatures $T > T_c^+ = T_c + 0$ where the system is already in the normal state, experiment has established the perplexing behavior

$$\alpha(T) = \alpha_0 + \alpha_1 T. \quad (1)$$

The *nonzero* offset $\alpha_0 \simeq 0.5 \times 10^{-5}/\text{K}$ exceeds those found in ordinary metals at these temperatures by a huge factor of order $10^3 - 10^4$. This implies that an analogous *classical-like* offset S_0 , associated with α_0 by the relation

$\alpha_0 = \partial S_0/\partial P$, is present in the entropy itself – pointing unambiguously to the presence of quantum chaos in the regime of extremely low temperatures $T \simeq T_c \ll T_D$.

Another experimental challenge is associated with the low-temperature, non-Fermi-liquid (NFL) behavior of the normal-state resistivity $\rho(T)$ of the same CeCoIn₅ metal at various pressures P , which, according to FL theory, should obey the formula $\rho(T) = \rho_0 + A_2 T^2$. Instead, at $P < P^* \simeq 2$ GPa, experiment [3] has revealed the *classical-like* strange-metal behavior

$$\rho(T) = \rho_0 + A_1 T, \quad (2)$$

shown in Fig. 1. It is as if classical physics already prevails at $T_c^+ < T \ll T_D$. This remarkable linear-in- T behavior of $\rho(T)$ is currently observed in diverse systems (see e.g. [4–6]). In some cases, the slope A_1 experiences a noticeable jump [7] (see below).

Even more bizarre behavior has surfaced in recent studies [8] of the resistivity of twisted bilayer graphene (TBLG) as a function of twist angle θ , as depicted in Fig. 2. Profound variations of $A_1(\theta)$ are seen, especially toward to the so-called magic angle θ_m , where the A_1 term increases by more than three orders of magnitude, as so does the residual resistivity $\rho_0(\theta)$, echoing a tenfold variation of ρ_0 as a function of pressure P , shown in Fig. 1. Since ρ_0 must be a parameter-independent quantity [9] if the impurity population remains unchanged, its documented behavior defies explanation within the standard FL approach.

Moreover, in high-temperature superconducting, overdoped copper oxides, where $T_c(x)$ terminates at critical doping value x_c , with nearly linear dependence on $x_c - x$ (see Fig. 3), the quite remarkable doping independence

$$A_1(x)/T_c(x) = \text{const}, \quad (3)$$

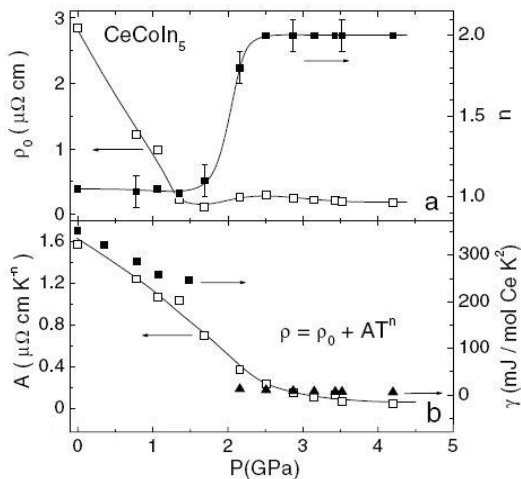


FIG. 1: Upper panel: Values of the residual resistivity ρ_0 (left axis, open squares) and the index n in the fit $\rho(T) = \rho_0 + AT^n$ (right axis, solid squares) versus pressure P . Bottom panel: Temperature coefficient of resistivity A (left panel, open squares) and specific-heat coefficient γ (right panel, solid squares and solid triangles). The authors thank J. D. Thompson for permission to present data published in Ref. [3].

has been discovered [10, 11], a feature shared with the Bechgaard salts [12]. As emphasized in Ref. [11], this feature points to the presence of a hidden phase, emergent at x_c *simultaneously* with the superconducting state.

Explanation of such strange-metal behavior (2) found at low $T_c^+ < T \ll T_D$ has become one of the most intensely debated theoretical problems of the modern condensed-matter theory. Analysis of proposed scenarios in a recent review article [13] has concluded that none of these is capable of explanation of all the relevant experimental findings. In particular, candidates based on a quantum-critical-point (QCP) scenario fall short. As witnessed by the phase diagrams of CeCoIn_5 , cuprates, and graphene, there are no appropriate ordered phases adjacent to the strange metal region; the effects of associated quantum fluctuations are, at best, small.

Existing theories having failed to explain the available experimental results, we turn to a different scenario, based specifically on the formation of a fermion condensate (FC), which does provide a basis for explanation of their NFL nature, including excess entropy with its implicit chaotic aspect. The possibility of this phenomenon was proposed 30 years ago [14]. At $T = 0$, it involves the emergence, in normal states of strongly correlated many-fermion systems, of an *interaction-induced* flat portion $\epsilon(\mathbf{p}) = 0$ of the single-particle spectrum $\epsilon(\mathbf{p})$ in the FC region $\mathbf{p} \in \Omega$, embracing the nominal Fermi surface. Within this regime, the quasiparticle momentum distribution (hereafter denoted $n_*(\mathbf{p})$) departs drastically from the Landau step $n_L(\mathbf{p}) = \theta(-\epsilon(\mathbf{p}))$. The analogy with a

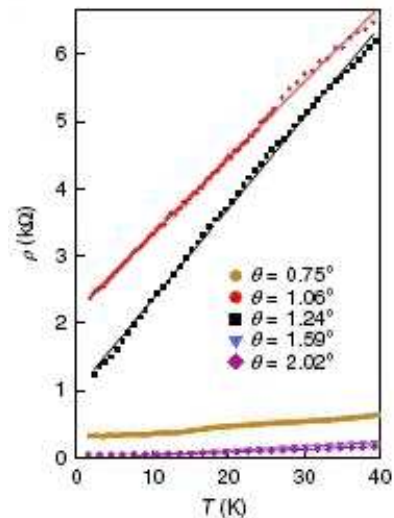


FIG. 2: NFL resistivity $\rho(T)$ measured in TBLG devices at different twist angles. The authors express their gratitude to A. F. Young for permission to present data published in Ref. [8].

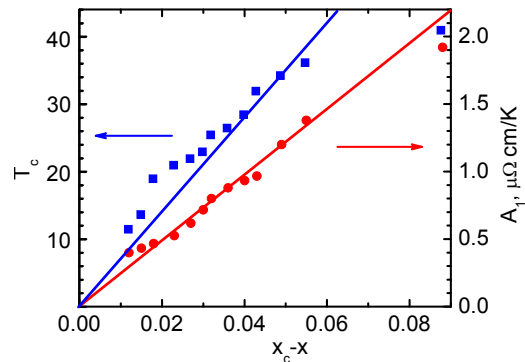


FIG. 3: Dependence of the factor A_1 in the resistivity $\rho(T)$ (red circles, right axis) and the critical temperature T_c (blue squares, left axis) of overdoped $\text{La}_{2-x}\text{Sr}_x\text{CuO}_4$ films on the doping x measured from its critical value $x_c = 0.26$ [10]. Red and blue lines show the best linear fits to the data, which support the conclusion that $A_1(x) \propto T_c(x)$, indicative of behavior inconsistent with conventional theory.

boson condensate (BC) is evident in the respective densities of states $\rho_{\text{FC}}(\epsilon) = n_{\text{FC}}\delta(\epsilon)$ and $\rho_{\text{BC}}(\epsilon) = n_{\text{BC}}\delta(\epsilon)$, where n_{FC} and n_{BC} denote the fermion and boson condensate densities.

Interaction-induced flat bands, responsible for intervention of chaotic behavior into the low-temperature region $T_c^+ < T \ll T_D$ emerge at critical points where the number of roots of equation $\epsilon(\mathbf{p}, n_L) = 0$ changes [15, 16]. Because no inherent symmetries of the initial ground state are lost beyond the associated bifurcation point, it is identified as a *topological critical point* (TCP)

at which the group velocity $|\nabla\epsilon(\mathbf{p})|$ can be shown to vanish. Accordingly, such TCPs *coincide* with associated van Hove singularities at which the density of states diverges [17, 18].

We begin the analysis with a key observation. Whereas the quasiparticle pattern of phenomena in conventional Fermi liquids created by Landau in his celebrated work [19] is duly recognized, its sequel [20], along with a related paper by Pitaevskii [21] still remain, to some extent, in the shadows. In these two works, a universal quantitative procedure for the renormalization of the basic equations of Fermi liquid (FL) theory was developed for evaluation of thermodynamic properties. Its implementation allows one, *irrespective of the strength of correlations*, to recast these equations in closed form, as if one were dealing with a *gas of interacting quasiparticles*. (The word "gas" is appropriate, since the final equations, such as Eq. (6), contain only the single phenomenological amplitude f of quasiparticle-pair collisions).

In *conventional* Fermi liquids as addressed in Refs. [20, 21], the quasiparticles are assumed to be immortal, in accord with the inherently small value of the ratio $\gamma/\epsilon(p)$. This allows one to write the pole part G_q of the single-particle Green function $G = (\epsilon - \epsilon_p^0 - \Sigma)^{-1}$ in the form

$$G_q(\mathbf{p}, \epsilon) = \frac{1 - n_L(\mathbf{p})}{\epsilon - \epsilon(\mathbf{p}) + i\delta} + \frac{n_L(\mathbf{p})}{\epsilon - \epsilon(\mathbf{p}) - i\delta}, \quad (4)$$

with infinitesimally small $\delta = +0$.

However, in later work of Abrikosov and Gor'kov [22, 23] on the theory of superconducting alloys, where $\gamma \ll T_F$ acquires a *finite* value due to impurity-induced scattering, the form of Landau's G_q changes to

$$G_q(\mathbf{p}, \epsilon) = \frac{1 - n_L(\mathbf{p})}{\epsilon - \epsilon(\mathbf{p}) + i\gamma} + \frac{n_L(\mathbf{p})}{\epsilon - \epsilon(\mathbf{p}) - i\gamma} \quad (5)$$

with $\gamma > 0$. Importantly, even though the ratio $\gamma/\epsilon(\mathbf{p})$ does exceed unity in these systems, the FL quasiparticle picture *remains valid*, and a *refined* version of the original FL theory based on Eq. (5) is still applicable [24].

Further alteration of Landau's pole part G_q occurs beyond the TCP where interaction-induced flat bands emerge. In this case, the damping γ comes into play within the framework of Eq. (5) to meet concerns voiced by Nozieres [25], with the necessary alteration of this expression reducing to the replacement of Landau's original FL quasiparticle occupation numbers $n_{\text{FL}}(\mathbf{p})$ with by new ones $n_*(\mathbf{p})$ characterizing the FC.

Importantly, the difference between n_{FL} and n_* resides solely in the FC region Ω , where n_* is to be determined through solution of the nonlinear integral equation of the theory of fermion condensation,

$$\frac{\partial\epsilon(\mathbf{p})}{\partial\mathbf{p}} = \frac{\partial\epsilon_0(\mathbf{p})}{\partial\mathbf{p}} + \left(f(\mathbf{p}, \mathbf{p}_1) \frac{\partial n_*(\mathbf{p}_1)}{\partial\mathbf{p}_1} \right), \quad (6)$$

its left side *vanishing identically* in this region.

Derivation of Eq. (6) and methods for its numerical solution will be addressed in the Supplementary Material. Here we focus on several pertinent aspects. The round brackets in Eq. (6) imply integration and summation over intermediate momenta and spins, while $f(\mathbf{p}, \mathbf{p}_1)$ stands for the spin-independent part of the Landau interaction function. The free term includes all contributions to the group velocity that remain in the $f = 0$ limit. In the TBLG problem, this term can be identified with that obtained in model flat-band calculations (e.g. Refs. [26, 27]) where the FL contribution was missing. However, in such a strongly correlated electron system such as graphene, the FL term is by no means small, and hence tends to trigger breakdown of the topological stability of the Landau state, leading to the advent of interaction-induced flat bands, rather than the near-flat bands found in Refs. [26, 27].

Eq. (6) is derived from the formal relation $\delta\Sigma = (\mathcal{U}\delta G)$ of variational many-body theory for the self-energy in terms of the subset of Feynman diagrams \mathcal{U} of the two-particle scattering amplitude that are irreducible in the particle-hole channel, hence regular near the Fermi surface. In doing so, two identities of many-body theory [28, 29] are combined. The first,

$$-\frac{\partial G^{-1}(\mathbf{p}, \epsilon)}{\partial\mathbf{p}} = \mathbf{p}/m_e - \left(\mathcal{U}(\mathbf{p}, \epsilon; \mathbf{k}, \omega) \frac{\partial G(\mathbf{k}, \omega)}{\partial\mathbf{k}} \right), \quad (7)$$

is derived assuming gauge invariance of the theory, where $\delta G(p, \epsilon) = G(\mathbf{p} - e\mathbf{A}, \epsilon) - G(p, \epsilon)$. The second,

$$\frac{\partial G^{-1}(\mathbf{p}, \epsilon)}{\partial\epsilon} \mathbf{p} = \mathbf{p} - \left(\mathcal{U}(\mathbf{p}, \epsilon; \mathbf{k}, \omega) \frac{\partial G(\mathbf{k}, \omega)}{\partial\epsilon} \mathbf{k} \right), \quad (8)$$

is derived in homogeneous matter exploiting the commutativity between the momentum operator \mathbf{p} and the total Hamiltonian of the system [29], where $\delta G(p, \epsilon) = G(p, \epsilon - \mathbf{p}\mathbf{V}) - G(p, \epsilon)$.

A salient feature of the regularization procedure formulated in Ref. [20] is that all the regular contributions to these identities can be absorbed into a new phenomenological two-particle scattering amplitude f , replacing the original quantity \mathcal{U} and thereby yielding Eq. (6). We stress that Eq. (7) holds *both* in conventional Fermi liquids *and* in electron systems of solids moving in the periodic external field of the crystal lattice. At the same time, in solids Eq. (8) receives corrections proportional to the gradient of the external field created by the crystal lattice. Such insignificant terms can be harmlessly included in the free term \mathbf{v}_0 . In short, the widespread impression that the FL approach is inapplicable for crystal structures is groundless.

We may recall that according to Ref. [25], the single-particle spectrum determined from Eq. (6) and properly generalized to nonzero temperatures acquires a small dispersion, linear in T ,

$$\epsilon(\mathbf{p}, T) = T \ln \frac{1 - n_*(\mathbf{p})}{n_*(\mathbf{p})}, \quad \mathbf{p} \in \Omega. \quad (9)$$

Experimental verification of this effect through ARPES measurements is crucial for substantiation of the FC concept under consideration.

The second distinctive signature of the FC phenomenon lies in the occurrence of a nonzero entropy excess S_* , emergent upon substituting the FC solution $n_*(\mathbf{p})$ into the familiar Landau formula for evaluation of the entropy, yielding [14, 30–32]

$$S_* = -2 \sum_{\mathbf{p}} [n_*(\mathbf{p}) \ln n_*(\mathbf{p}) + (1 - n_*(\mathbf{p})) \ln(1 - n_*(\mathbf{p}))], \quad (10)$$

and, in turn, an NFL nonzero value α_* of the coefficient of thermal expansion. Because the presence of a nonzero S_* would contradict the Nernst theorem $S(T=0) = 0$ if it survived to $T=0$, the FC must inevitably disappear [14, 31, 32] at some very low T . One well-elaborated scenarios for this metamorphosis is associated with the occurrence of phase transitions, such as the BCS superconducting transition emergent in the case of attraction forces in the Cooper channel, or an antiferromagnetic transition, typically replacing the superconducting phase in external magnetic fields H exceeding the critical field H_{c2} .

At $H < H_{c2}$, a nonzero BCS gap $\Delta(0)$ in the single-particle spectrum $E(\mathbf{p}) = \sqrt{\epsilon^2(\mathbf{p}) + \Delta^2}$ does provide for nullification of $S(T=0)$. This scenario applies in systems that host the FC as well, opening a specific route to high- T_c superconductivity [14, 33, 34]. Indeed, consider the BCS equation for determining T_c :

$$D(\mathbf{p}) = -2 \int \mathcal{V}(\mathbf{p}, \mathbf{p}_1) \frac{\tanh \frac{\epsilon(\mathbf{p}_1, T_c)}{2T_c}}{2\epsilon(\mathbf{p}_1, T_c)} D(\mathbf{p}_1) dv_1. \quad (11)$$

Here $D(\mathbf{p}) = \Delta(\mathbf{p}, T \rightarrow T_c) / \sqrt{T_c - T}$ plays the role of an eigenfunction of this linear integral equation, while $\mathcal{V}(\mathbf{p}, \mathbf{p}_1)$ is the block of Feynman diagrams for the two-particle scattering amplitude that are irreducible in the Cooper channel. Upon insertion of Eq. (9) into this equation and straightforward momentum integration over the FC region, one arrives at a non-BCS *linear* relation

$$T_c(x) \simeq \lambda \eta(x) T_F, \quad (12)$$

where λ is the effective pairing constant and $\eta(x)$ the FC density, behavior in accord with the experimental Uemura plot [35, 36].

As discussed above, the entropy excess $S_* \propto \eta$ comes into play at temperatures $T_c^+ < T_c \ll T_D$ so as to invoke a T -independent term α_0 in the coefficient of thermal expansion, which, in that regime, serves as a signature of fermion condensation [31, 32]. Accordingly, execution of extensive low- T measurements of the thermal expansion coefficients in candidate materials would, in principle, provide means (i) to distinguish between flat bands that do not entail excess entropy S_* and the interaction-induced exemplars, and (ii) to create a database of systems that exhibit pronounced NFL properties, in aid of searches for new unconventional superconductors.

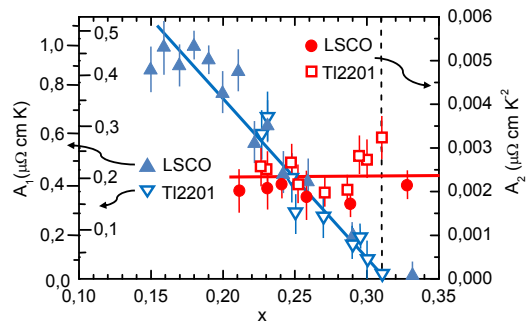


FIG. 4: Doping dependence of the coefficients A_1 and A_2 for overdoped LSCO films and Tl2201 compounds. Left axis: triangles indicate experimental data [11] on A_1 for LSCO (scale outside) and Tl2201 (scale inside), while the straight line reproduces the FC scenario prediction $A_1 \propto (x_c - x)$, with $x_c \simeq 0.3$ and a coefficient A chosen to fit the average trend. Right axis: full circles and empty squares show corresponding experimental data [11] on A_2 for LSCO and Tl2201, while the horizontal straight line represents the prediction $A_2 \simeq \text{const}$ [42] through the critical point.

Very recently, the FC scenario has gained tentative support from ARPES measurements performed in monolayer graphene intercalated by Gd, which have revealed the presence of a flat portion in the single-particle spectrum [37]. However, verification of the correspondence between the flat bands detected in the bilayer system TBLG [8, 26, 27, 36, 38–40] and the interaction-driven variety considered here requires a concerted analysis of kinetic properties, especially of comprehensive experimental data on the low T resistivity $\rho(T) = \rho_0 + A_1 T + A_2 T^2$.

Numerous theoretical studies of the NFL behavior of $\rho(T)$ based on the FC concept have been performed. Directing the reader to Refs. [32, 41, 42] for details, we summarize their pertinent results in the relation

$$\rho_0(x, P) = \rho_i + a_0 T_F \eta^2(x, P), \quad A_1(x, P) = \frac{a_1}{2e^2 T_F} \eta(x, P), \quad (13)$$

where ρ_i is the impurity-induced part of ρ and a_0, a_1 are numerical factors. This expression properly explains the data shown in Figs. 1 and 2. Indeed, we see that in systems having a FC, the residual resistivity ρ_0 depends critically on the FC density η , which changes under variation of input parameters such as pressure P and doping x – an effect that is missing in a popular scenario for Planckian dissipation [43–46].

Comparison of Eq. (13) with Eq. (12) shows that the theoretical ratio $A_1(x)/T_c(x)$ is indeed doping-independent, in agreement with the challenging experimental results shown in Fig. 3. Moreover, assuming that the FC parameter $\eta(x)$ varies linearly with $x_c - x$, which is compatible with model numerical calculations based on Eq. (6), the corresponding result obtained from Eq. (13) is consistent with the data shown in Fig. 4.

Returning to the issue of classical-like Planck dissipation, it is worth noting that such a feature exists as well [47] in the FC scenario for NFL behavior of $\rho(T)$ of cuprates and graphene. It transpires that in these systems a specific collective mode, transverse zero-sound (TZS), emerges in domains of their phase diagrams where the ratio m^*/m of effective mass to bare mass is in excess of 6 [28, 48] (cf. data on CeCoIn₅ where this ratio is of order 10^2 [44]). In the common case where the Fermi surface is multi-connected, some branches of the TZS mode turn out to be damped, thereby ensuring the occurrence of a linear-in- T term in the resistivity $\rho(T)$, broadly analogous to the situation that arises for electron-phonon scattering in solids in the classical limit $T > T_D$. (Supplementary Material will provide details). As a result, FC theory predicts that a break will occur in the straight line $\rho(T) = \rho_0 + A_1T$ at some characteristic Debye temperature T_{TZS} [41, 49], in agreement with experimental data on Sr₃Ru₂O₇ [44]. However, in unconventional superconductors, the situation changes provided $T_{TZS} < T_c$, since this break then disappears, and the behavior of the resistivity $\rho(T)$ at $T_c^+ < T \ll T_D$ is fully reminiscent of that in classical physics, as is observed in CeCoIn₅ [3] and in TBLG (M4 device) [40].

In conclusion, we have outlined a theory of prominent NFL phenomena observed in strongly correlated electron systems within the scenario of interaction-induced flat bands. Emphasis is given to manifestations of topological quantum chaos at temperatures T far below the classical Debye value. It was demonstrated that the predictions of this theory are consistent with the challenging experimental findings, including those represented in Figs. 1-4.

We are grateful to H. Aoki, P. Esquinazi, P. Gegenwart, M. Greven, E. Henriksen, M. Katsnelson, Ya. Kopelevich, S. Kravchenko, Z. Nussinov, F. Steglich, V. Shaginyan, J. D. Thompson and G. Volovik for fruitful discussions. VAK and JWC acknowledge financial support from the McDonnell Center for the Space Sciences.

-
- [1] N. Oeschler et al., Phys. Rev. Lett. **91**, 076402 (2003).
 [2] J. G. Donath et al., Phys. Rev. Lett. **100**, 136401 (2008).
 [3] V. A. Sidorov et al., Phys. Rev. Lett. **89**, 157004 (2002).
 [4] H. v. Löchneysen et al., Rev. Mod. Phys. **79**, 1015 (2007).
 [5] M. Shubert, H. S. Jeevan, P. Gegenwart, J. Phys. Soc. Japan, **80**, SA004 (2011) and references therein.
 [6] L. Taillefer, Annu. Rev. Condens. Matter Phys. **1**, 51 (2010).
 [7] A. W. Rost et al., Proc. Natl. Acad. Sci. USA **108**, 16549 (2011).
 [8] G. Polshyn et al., Nature Physics **15**, 1101 (2019).
 [9] E. M. Lifshitz, L. P. Pitaevskii, *Physical Kinetics*, Eq. (78.17) (Elsevier, Amsterdam, 1981).
 [10] I. Bozović et al., Nature **536**, 309 (2016).
 [11] R. A. Cooper et al., Science **323**, 603 (2009).
 [12] N. Doiron-Leyraud et al., Phys. Rev. B **80**, 214531 (2010).
 [13] B. Keimer et al., Nature **518**, 179 (2015).
 [14] V. A. Khodel, V. R. Shaginyan, JETP Lett. **51**, 553 (1990).
 [15] I. M. Lifshitz, Sov. Phys. JETP **11**, 1130 (1960).
 [16] G. E. Volovik, JETP Lett. **53**, 222 (1991); Springer Lecture Notes in Physics **718**, 31 (2007).
 [17] G. E. Volovik, JETP Lett. **59**, (83) (1994).
 [18] V. Yu. Irkhin, A. A. Katanin, M. I. Katsnelson, Phys. Rev. Lett. **89**, 076401 (2002).
 [19] L. D. Landau, Zh. Exp. Teor. Fiz. **30**, 1058 (1956); Sov. Phys. JETP **3**, 920 (1957).
 [20] L. D. Landau, Zh. Exp. Teor. Fiz. **35**, 97 (1958); Sov. Phys. JETP **8**, 70 (1959).
 [21] L. P. Pitaevskii, Zh. Exp. Teor. Fiz. **37**, 1794 (1959); Sov. Phys. JETP **10**, 1267 (1960).
 [22] A. A. Abrikosov, L. P. Gor'kov, Sov. Phys. JETP **12**, 1243 (1960).
 [23] L. P. Gor'kov, *Theory of Superconducting Alloys*, edited by K. H. Bennemann and J. B. Kettelson, Superconductivity Vol. 1 (Springer-Verlag, New York, 2008).
 [24] V. A. Khodel, J. W. Clark, M. V. Zverev, Phys. Rev. B **99**, 184503 (2019).
 [25] P. Nozières, J. Phys. I France **2**, 443 (1992).
 [26] E. S. Morell et al., Phys. Rev. B **82**, 121407 (2010).
 [27] R. Bistritzer, A. H. McDonald, Proc. Natl. Acad. Sci. **108**, 12233 (2011).
 [28] A. A. Abrikosov, L. P. Gor'kov, I. Ye. Dzyaloshinskii, *Quantum Field Theoretical Methods in Statistical Physics* (Pergamon Press, Oxford, 1965).
 [29] A. B. Migdal, *Theory of Finite Fermi Systems and Applications to Atomic Nuclei* (Wiley, New York, 1967).
 [30] V. A. Khodel, J. W. Clark, M. V. Zverev, Phys. Rev. B **78**, 075120 (2008).
 [31] J. W. Clark, M. V. Zverev, V. A. Khodel, Ann. Phys. **327**, 3063 (2012).
 [32] V. R. Shaginyan et al., Phys. Rev. B **86**, 085147 (2012).
 [33] N. B. Kopnin, T. T. Heikkilä, G. E. Volovik, JETP Lett. **94**, 233 (2011).
 [34] G. E. Volovik, JETP Lett. **53**, 222 (2018).
 [35] T. Uemura, J. Phys. Condens. Matter, **16**, S4515 (2004).
 [36] Y. Cao et al., Nature **556**, 43 (2018).
 [37] S. Link et al., Phys. Rev. B **100**, 121407(R) (2019).
 [38] M. Yankovitz et al., Science **363**, 1059 (2018).
 [39] Y. Cao et al., Nature **556**, 80 (2018).
 [40] Y. Cao et al., Phys. Rev. Lett. **124**, 076801 (2020).
 [41] V. R. Shaginyan, K. G. Popov, V. A. Khodel, Phys. Rev. B **88** 115103 (2013).
 [42] V. A. Khodel, J. W. Clark, M. V. Zverev, Phys. Lett. A **382**, 3281 (2018).
 [43] J. Zaanen, Nature **430**, 512 (2004).
 [44] J. A. N. Bruin et al., Science **339**, 804 (2013).
 [45] A. Legros et al., Nature Phys. **14** (2018).
 [46] A. A. Patel, S. Sachdev, Phys. Rev. Lett. **123**, 066601 (2019).
 [47] V. A. Khodel, J. W. Clark, M. V. Zverev, Physics of Atomic Nuclei **74**, 1237 (2011).
 [48] I. M. Halatnikov, *An Introduction to the Theory of Superfluidity* (Benjamin, New York, 1965).
 [49] V. R. Shaginyan et al., JETP Lett. **110**, 290 (2019).

SUPPLEMENTARY MATERIAL

”Onset of topological quantum chaos in strongly correlated electron systems”

1. Onset of chaos with fermion condensation: an elemental example

The relationship of fermion condensation to chaotic phenomena as understood in classical physics has been expressed so far in terms of the existence of a non-zero zero-point entropy associated with chaotic behavior of scattering processes. The correspondence with familiar treatments of classical chaos [1–4] can be made more transparent by the following simple but fundamental example.

Superdense quark-gluon plasma (QGP) is unique among quantum many-body systems in that the topological rearrangement of the Landau state leading to a fermion condensate already occurs in first-order perturbation theory, which yields a schematic single-particle spectrum

$$\epsilon(p) - \mu = v_F(p - p_F) + a(p - p_F) \ln(p - p_F). \quad (14)$$

This result is reminiscent of the single-particle spectrum of a homogeneous Coulomb plasma, with a crucial difference: the QGP parameter a carries a *positive* sign, due to the attractive character of quark-gluon exchange, leading to an infinite *negative* slope of the spectrum $\epsilon(p)$ at the Fermi momentum $p = p_F$. As demonstrated in the iterative procedure applied by Pethick, Baym, and Monien (PBM) for solution of Eq. (14), this difference has phenomenal consequences, giving rise to unlimited breeding of new sheets of the Fermi surface [5].

The same PBM Fermi-sheet proliferation persists in a more accurate evaluation of the QGP spectrum based on the Dyson equation [6]

$$\epsilon(p) = \epsilon_p^0 + g \int \ln \frac{1}{|p - p_1|} n(p_1) dp_1, \quad (15)$$

where $\epsilon_p^0 \simeq cp$ is the bare spectrum with c the velocity of light, $g > 0$ is an effective coupling constant, and $n(p)$ is the corresponding quasiparticle momentum distribution.

Since an attempt at straightforward iterative solution of Eq. (15) fails, an alternative approach was applied in Ref. [6]. As outlined below, the problem was reformulated in terms of an iterative discrete-time map, in analogy with classical studies of chaos, with subsequent time-averaging of relevant quantities. The salient feature of the resulting self-consistent solution of Eq. (15) is the development of an interaction-induced flat portion in the single-particle spectrum $\epsilon(p)$, embracing the nominal Fermi surface. Analogous nearly-flat low-energy bands, with extremely low values of the Fermi velocity v_F , have become commonplace in condensed-matter

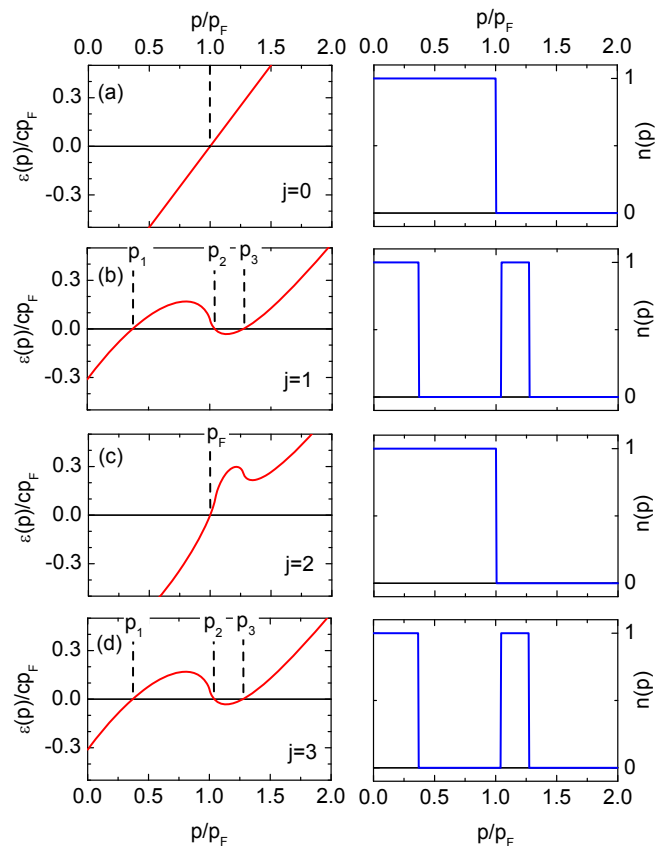


FIG. 5: Iterative maps for Eq. (15) with the dimensionless parameter g/c set to unity. The left-hand panels show iterations for the spectrum $\epsilon^{(j)}(p)$ in units of cp_F for $j = 0, 1, 2, 3$ (these iterations being reckoned from the corresponding iterations for the chemical potential), while the right-hand panels show iterations for the momentum distributions $n^{(j)}(p)$.

physics, typified by those studied theoretically in twisted bilayer graphene [7].

In the standard iterative scheme, the j th iteration $n^{(j)}(p)$, with $j = 0, 1, 2, \dots$, is inserted into the right side of Eq. (15) to generate the next iteration of the single-particle spectrum, $\epsilon^{(j+1)}(p)$, measured now from the chemical potential μ , and this process is repeated indefinitely. As seen in Fig. 1, the divergence of the slope of $\epsilon^{(0)}(p)$ leads originally to a specific 2-cycle in which all even iterations coincide with the Landau momentum distribution $n_{FL}(p) = \theta(p_F - p)$. Coincidence occurs in all odd iterations as well; however, their structure differs from that of the Landau state by the presence of a break in $n_{FL}(p)$. In principle, this cycle is eliminated in a more sophisticated iterative scheme in which the neighboring iterations are mixed with each other [6, 8]. However, such a refinement does not lead to convergence.

To overcome this difficulty it is beneficial to introduce discrete time-steps numbered j at which the functions $\epsilon(p, t)$ and $n(p, t)$ are updated, the latter undergo-

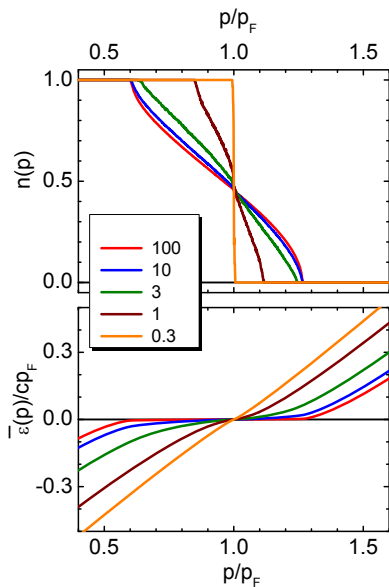


FIG. 6: Single-particle spectrum (upper panel) and momentum distribution (lower panel) averaged according to (16). Correspondence between the color of lines and the number of effective iterations $N\zeta$, the product of the number of real iterations N , and the parameter of mixing of neighboring iterations ζ , is indicated.

ing chaotic jumps from 0 to 1 and vice-versa as j and hence t increases. A further adjustment makes the crucial difference. Aided by formulas adapted from classical mechanics, $\epsilon(p, t)$ and $n(p, t)$ are replaced, respectively, by an averaged single-particle spectrum $\bar{\epsilon}(p)$ and a corresponding averaged occupation number $\bar{n}(p)$:

$$\bar{\epsilon}(p) = \lim_{\tau \rightarrow \infty} \frac{1}{\tau} \int_0^{\tau} \epsilon(p, t) dt = \lim_{N \rightarrow \infty} \frac{1}{N} \sum_0^N \epsilon^{(j)}(p),$$

$$\bar{n}(p) = \lim_{\tau \rightarrow \infty} \frac{1}{\tau} \int_0^{\tau} n(p, t) dt = \lim_{N \rightarrow \infty} \frac{1}{N} \sum_0^N n^{(j)}(p) \quad (16)$$

Importantly, Eq. (15) holds if one inserts the time-averaged quantities $\bar{\epsilon}(p)$ and $\bar{n}(p)$ instead of the original ones.

Results from calculations demonstrating emergence of the interaction-induced flat bands of the QGP are displayed in Fig. 2. As seen, the function $\epsilon(p)$ does vanish identically in a momentum region Ω where the 2-cycle originally sets in, while the quasiparticle momentum distribution, denoted by $n_*(p)$, emerges as a *continuous* function of p in this region.

2. Equality of quasiparticle and particle numbers in strongly correlated Fermi systems

In this section we outline a quasiparticle formalism

free of the Landau restriction $\gamma/\epsilon(p) \ll 1$, where γ represents the damping of single-particle excitations and ϵ their energy. In strongly correlated electron systems such as graphene, the Landau quasiparticle picture is putatively inapplicable, since the ratio γ/ϵ is known not to be small, in contrast to requirements of the original Landau theory [9–11]. However, we shall find that smallness of this ratio is a sufficient, but not necessary, condition for validity of the quasiparticle pattern. Indeed, in superconducting alloys, the quasiparticle formalism is operative (cf. the textbook [12] and/or Ref. [13]), despite the fact that γ/ϵ greatly exceeds unity due to the presence, in γ , of a term arising from energy-independent impurity-induced scattering. Moreover, the actual requirement for validity of the quasiparticle method hinges on the smallness of the damping γ compared with the *Fermi energy* T_F . Consequently,

- In correlated homogeneous Fermi liquids, the particle number always coincides with the quasiparticle number, *irrespective* of the magnitude of the damping of single-particle excitations, as long as $\gamma \ll T_F$.

Proof of this statement is based on the dichotomy characterizing the impact of long-wave external fields $V(\mathbf{k} \rightarrow 0, \omega \rightarrow 0)$ on correlated Fermi systems, which depends crucially on the ratio ω/k . Indeed, due to the fictitious character of coordinate-independent external fields $V(k=0, \omega)$, no physical change of the system occurs upon their imposition. On the contrary, change does ensue in the opposite case of static fields $V(k, \omega=0)$, its principal effect being expressed in the pole parts G_q of the Green functions G .

By way of illustration, in what follows we adopt a pole part of the form

$$G_q(p, \epsilon) = (\epsilon - \epsilon(p) + i\gamma \text{sgn}(\epsilon))^{-1}, \quad (17)$$

with $\gamma > 0$, as introduced by Abrikosov and Gor'kov in their theory of superconducting alloys [14, 15]. However, the final results are invariant with respect to the explicit form of G_q .

Further, in the ensuing analysis it is instructive to represent the quasiparticle density n as an integral

$$n = -\frac{2}{3} \iint p_n \frac{\partial G_q(p, \epsilon)}{\partial p_n} \frac{d^3 \mathbf{p} d\epsilon}{(2\pi)^4 i}, \quad (18)$$

where p_n is the momentum component normal to the Fermi surface. Here, integration over energy is assumed to be performed before differentiation with respect to momentum p . The correct result is also obtained provided the derivative $\partial G_q/\partial p_n$ in the integrand of Eq. (18) is rewritten in the form

$$\frac{\partial G_q(p, \epsilon)}{\partial p_n} = -\lim_{\mathbf{k} \rightarrow 0} G_q(\mathbf{p}, \epsilon) G_q(\mathbf{p} + \mathbf{k}, \epsilon) \frac{\partial G_q^{-1}(p, \epsilon)}{\partial p_n}, \quad (19)$$

yielding

$$n = \frac{2}{3} \iint p_n \lim_{\mathbf{k} \rightarrow 0} G_q(\mathbf{p}, \varepsilon) G_q(\mathbf{p} + \mathbf{k}, \varepsilon) \frac{\partial G_q^{-1}(p, \varepsilon)}{\partial p_n} \frac{d^3 \mathbf{p} d\varepsilon}{(2\pi)^{4i}}. \quad (20)$$

Evidently, integration over energy in Eq. (20) produces a nonzero result only if the poles of $G(\mathbf{p}, \varepsilon)$ and $G(\mathbf{p} + \mathbf{k}, \varepsilon)$ lie on opposite sides of the energy axis. This requirement is met provided the energies $\varepsilon(p)$ and $\varepsilon(\mathbf{p} + \mathbf{k})$ have opposite signs, so as to generate the relevant factor $(dn(p)/d\varepsilon(p))(d\varepsilon(p)/dp_n) \equiv dn(p)/dp_n$ in the integration over energy. The analogous relation

$$\rho = \frac{2}{3} \iint p_n \lim_{\mathbf{k} \rightarrow 0} G(\mathbf{p}, \varepsilon) G(\mathbf{p} + \mathbf{k}, \varepsilon) \frac{\partial G^{-1}(p, \varepsilon)}{\partial p_n} \frac{d^3 \mathbf{p} d\varepsilon}{(2\pi)^{4i}} \quad (21)$$

applies for the total density ρ .

Hereafter we adopt symbolic notations frequently employed in Fermi Liquid (FL) theory. With round brackets implying summation and integration over all intermediate variables and the normalization factor $1/(2\pi)^{4i}$, Eqs. (18) and (21) then become

$$n = \frac{2}{3} \left(p_n G_q G_q \frac{\partial G_q^{-1}}{\partial p_n} \right), \quad \rho = \frac{2}{3} \left(p_n G G \frac{\partial G^{-1}}{\partial p_n} \right). \quad (22)$$

Following Pitaevskii [11], we exploit two generic identities of many-body theory. The first of these,

$$-\frac{\partial G^{-1}(p, \varepsilon)}{\partial p_n} = \frac{p_n}{m} + \left(\mathcal{U}(p, k) \frac{\partial G(k, \omega)}{\partial k_n} \right), \quad (23)$$

where \mathcal{U} represents the block of Feynman diagrams for the scattering amplitude that are irreducible in the particle-hole channel, is derived assuming gauge invariance of the theory [12]. The second, of the form

$$\frac{\partial G^{-1}(p, \varepsilon)}{\partial \varepsilon} p_n = p_n + \left(\mathcal{U}(p, k) \frac{\partial G(k, \varepsilon)}{\partial \varepsilon} k_n \right), \quad (24)$$

stems from the commutativity of the momentum operator with the total Hamiltonian of the system [16].

The first step in the proof of the equality $\rho = n$ relies on Landau's decomposition of the product of two single-particle Green functions into a sum of terms,

$$\lim_{\mathbf{k} \rightarrow 0} G(\mathbf{p}, \varepsilon) G(\mathbf{p} + \mathbf{k}, \varepsilon) = z^2 A(p, \varepsilon) + B(p, \varepsilon), \quad (25)$$

in which B is a part of the limit regular near the Fermi surface, while the remaining quasiparticle propagator,

$$A(p, \varepsilon) = \lim_{\mathbf{k} \rightarrow 0} G_q(\mathbf{p}, \varepsilon) G_q(\mathbf{p} + \mathbf{k}, \varepsilon), \quad (26)$$

involves the quasiparticle weight $z = (1 - \partial \Sigma(p, \varepsilon)/\partial \varepsilon)^{-1}$ in the single-particle state. Evidently, integration over energy in this equation produces a nonzero result only if the poles of $G(\mathbf{p}, \varepsilon)$ and $G(\mathbf{p} + \mathbf{k}, \varepsilon)$ lie on opposite sides of the energy axis. This requirement is met provided the

energies $\varepsilon(p)$ and $\varepsilon(\mathbf{p} + \mathbf{k})$ have opposite signs, so as to generate the relevant factor $(dn(p)/d\varepsilon(p))(d\varepsilon(p)/dp_n) \equiv dn(p)/dp_n$ in the integration over energy.

It should be emphasized that there exists an important formula [10, 12] analogous to Eq. (26), namely

$$\begin{aligned} \frac{\partial G(p, \varepsilon)}{\partial \varepsilon} &= - \lim_{\omega \rightarrow 0} G(p, \varepsilon) G(p, \varepsilon + \omega) \frac{\partial G^{-1}(p, \varepsilon)}{\partial \varepsilon} \\ &\equiv -B(p, \varepsilon) \frac{\partial G^{-1}(p, \varepsilon)}{\partial \varepsilon}. \end{aligned} \quad (27)$$

Evidently, the result of integration of this expression over energy vanishes identically, since poles of the product $G(p, \varepsilon) G(p, \varepsilon + \omega)$ lie on the same side of the energy axis. Further, one finds that regular contributions to the key relations involved come from both the regular parts B of the product GG and the block \mathcal{U} itself.

The key step in the regularization procedure developed by Landau then lies in the introduction of a specific interaction amplitude Γ^ω determined by the equation

$$\Gamma^\omega = \mathcal{U} + \left(\mathcal{U} B \Gamma^\omega \right) \equiv \mathcal{U} + \left(\Gamma^\omega B \mathcal{U} \right), \quad (28)$$

which is capable of absorbing all the regular contributions, *irrespective* of the explicit form of the propagator A . Indeed, let us multiply both members of Eq. (23) from the left by the product $\Gamma^\omega B$, integrate over all variables and eliminate the expression $\Gamma^\omega B \mathcal{U}$ in the last term with the aid of Eq. (28), yielding finally

$$\begin{aligned} - \left(\Gamma^\omega(p, k) B(k, \varepsilon) \frac{\partial G^{-1}(k, \varepsilon)}{\partial k_n} \right) &= \left(\Gamma^\omega(p, k) B(k, \varepsilon) \frac{k_n}{m} \right) \\ &+ \left(\Gamma^\omega(p, k) \frac{\partial G(k, \varepsilon)}{\partial k_n} \right) - \left(\mathcal{U}(p, k) \frac{\partial G(k, \omega)}{\partial k_n} \right). \end{aligned} \quad (29)$$

Simple algebraic transformations then lead to the relation

$$-\frac{\partial G^{-1}(p, \varepsilon)}{\partial p_n} = \frac{\partial G^{-1}(p, \varepsilon)}{\partial \varepsilon} \frac{p_n}{m} - \left(z^2 \Gamma^\omega A \frac{\partial G^{-1}(k, \omega)}{\partial k_n} \right). \quad (30)$$

In obtaining this result, we have employed the equation [11, 12, 16]

$$\frac{\partial G^{-1}(p, \varepsilon)}{\partial \varepsilon} p_n = p_n + \left(\Gamma^\omega B k_n \right). \quad (31)$$

Near the Fermi surface, the relevant derivatives of G^{-1} are evaluated in terms of the corresponding derivatives of the pole part G_q^{-1} to obtain

$$-\frac{\partial G_q^{-1}(p, \varepsilon)}{\partial p_n} = \frac{\partial G_q^{-1}(p, \varepsilon)}{\partial \varepsilon} \frac{p_n}{m} + \left(z^2 \Gamma^\omega \frac{\partial G_q(k, \omega)}{\partial k_n} \right). \quad (32)$$

Significantly, integration over energy is obviated due to the presence of the Fermi surface, providing the structure of the pole term G_q given by Eq. (17).

Thus, in homogeneous matter, we are led to a Pitaevskii-style equation

$$\frac{\partial \epsilon(p)}{\partial p_n} = \frac{p_n}{m} + \left(f \frac{\partial n_*(k)}{\partial k_n} \right), \quad (33)$$

where the Landau notation $f = z^2 \Gamma^\omega$ is introduced. We emphasize that the sole condition employed has been the smallness of the ratio $\gamma/T_F \ll 1$.

Beyond the critical point where the topological stability of the Landau state breaks down, the momentum distribution $n_*(p)$ acquires the non-Fermi-Liquid (NFL) form found from numerical solution of this equation. With regard to TBLG and similar electron systems, the first term on the right side of this equation must be improved, which has been done e.g. in Ref. [7].

To prove the coincidence $\rho = n$, we multiply both sides of Eq. (30) from the left by the product $p_n B$ and integrate over all intermediate variables. Exploiting the fact that the integral $\left(B \partial G^{-1}(p, \varepsilon) / \partial \varepsilon \right) \equiv -\left(\partial G(p, \varepsilon) / \partial \varepsilon \right)$ vanishes identically in integrating over the energy, while observing that the remaining term involving the product $p_n B \Gamma^\omega$ simplifies with the aid of relation (31), we are led to

$$\begin{aligned} \left(p_n B \frac{\partial G^{-1}(p, \varepsilon)}{\partial p_n} \right) &= \left(p_n B z^2 \Gamma^\omega A \frac{\partial G^{-1}(k, \varepsilon)}{\partial k_n} \right) \\ &= z^2 \left(p_n A \frac{\partial G^{-1}(p, \varepsilon)}{\partial \varepsilon} \frac{\partial G^{-1}(p, \varepsilon)}{\partial p_n} \right) \\ &\quad - z^2 \left(p_n A \frac{\partial G^{-1}(p, \varepsilon)}{\partial p_n} \right). \end{aligned} \quad (34)$$

Transfer of the last term in Eq. (34) to the left side of this equation and further straightforward manipulation of the relation obtained leads us finally to

$$\rho = \frac{2}{3} \left(p_n G_q(p, \varepsilon) G_q(p, \varepsilon) \frac{\partial G_q^{-1}(p, \varepsilon)}{\partial p_n} \right) = n, \quad (35)$$

thereby establishing the coincidence of particle and quasi-particle numbers, independently of the magnitude of the damping of single-particle excitations. In the end, all that matters is the presence of the Fermi surface.

The final result $\rho = n$ is not sensitive to the explicit form of the quasiparticle propagator A . Consequently, it can be understood that the equality between particle and quasiparticle numbers generalizes to Fermi systems having Cooper pairing with a BCS gap function $\Delta(\mathbf{p})$. In that case it takes the form

$$\rho = n = 2 \sum_{\mathbf{p}} v^2(\mathbf{p}) \equiv 2 \sum_{\mathbf{p}} \left(\frac{1}{2} - \frac{\epsilon(\mathbf{p})}{\sqrt{\epsilon^2(\mathbf{p}) + \Delta^2(\mathbf{p})}} \right) \quad (36)$$

irrespective of the structure of the single-particle spectrum, thereby allowing for the presence of flat bands

and/or damping of normal-state single-particle excitations. This statement, best proved within the framework of the Nambu formalism along the same lines as before, provides the hitherto missing element of the FL approach to theory of strongly correlated superconducting Fermi systems.

3. New branches of the collective spectrum and low- T kinetic properties of strongly correlated electron systems

Here we discuss consequences stemming from the occurrence of additional branches of collective excitations in strongly correlated electron systems of solids [17, 18] whose presence is associated with a substantial enhancement of the effective mass m^* – often exceeding $10^2 m_e$ as in heavy fermion metals CeCoIn₅ [19]. Primarily, one is dealing with the transverse zero sound emergent when the first dimensionless harmonic of the Landau interaction function satisfies $F_1 = f_1 p_F m^* / \pi^2 > 6$ [20].

We briefly outline results from Ref. [18], in which a standard assumption on the arrangement of the Fermi surface is adopted. It is assumed to consist of two sheets, one containing light carriers whose Fermi velocity $v_L \simeq p_F / m_e$ greatly exceeds that of the heavy carriers populating the second band, $v_H = p_F / m^*$. In such systems, there exist several branches of transverse zero sound. Here we focus on a mode whose velocity is smaller than the Fermi value v_L . In this case, the dispersion relation yielding the complex value of its velocity $c = c_R + i c_I$ takes the form [18]

$$\begin{aligned} 1 &= \frac{F_1}{6} \left[1 - 3 \left(\frac{c^2}{v_H^2} - 1 \right) \left(\frac{c}{2v_H} \ln \frac{c + v_H}{c - v_H} - 1 \right) \right] \\ &\quad + \frac{F_1 v_H}{6 v_L} \left[1 - 3 \left(\frac{c^2}{v_L^2} - 1 \right) \left(\frac{c}{2v_L} \ln \frac{c + v_L}{c - v_L} - 1 \right) \right]. \end{aligned} \quad (37)$$

The imaginary part of the expression on the right side of this equation vanishes identically. As is easily verified, its real part comes primarily from the first term in the square brackets on the right-hand side, since the second term is suppressed by presence of the small factor v_H/v_L . In the realistic case $F_1 \gg 1$, we arrive after some algebra [18] at the result

$$c_R \propto v_L \sqrt{\frac{m_e}{m^*}}, \quad c_I \propto v_L \frac{m_e}{m^*}. \quad (38)$$

Thus we see that in strongly correlated electron systems, there is no ban on emission and absorption of the transverse zero-sound quanta, by virtue of the condition $c_R/v_L < 1$. This allows one to study the associated collision term along the same lines as in the familiar case of electron-phonon interactions in solids, where the resistivity $\rho(T)$ varies linearly with T provided $T > T_D$.

Additionally, the velocity c_R typically turns out to be smaller than the phonon velocity. This becomes the essential factor, especially in the case where the relevant Debye temperature becomes lower than T_c and kinetic properties of the normal states then obey classic laws in the whole temperature region.

-
- [1] H. Poincaré, *Les Methodes Nouvelles de la Mecanique Celeste* (Dover, New York, 1957).
- [2] M. Feigenbaum, *J. Stat. Phys.* **19**, 25 (1978).
- [3] R. M. May, *Nature* **261**, 459 (1976).
- [4] L. Reichl, *The Transition to Chaos*, 2nd Ed. (Springer-Verlag, Berlin, 2004).
- [5] C. J. Pethick, G. Baym, and H. Monien, *Nucl. Phys. A* **498**, 313 (1989) (see Eq. (19)).
- [6] V. A. Khodel, J. W. Clark, M. V. Zverev, *Phys. Rev. B* **78**, 075120 (2008).
- [7] R. Bistritzer, A. H. McDonald, *Proc. Natl. Acad. Sci. USA* **108** (30), 12233 (2011).
- [8] V. A. Khodel, M. V. Zverev, S. S. Pankratov, J. W. Clark, *Physics of Atomic Nuclei* **72**, 1382 (2009).
- [9] L. D. Landau, *ZhETF*, **30**, 1058 (1956); *Sov. Phys. JETP* **3**, 920 (1957).
- [10] L. D. Landau, *ZhETF*, **35**, 97 (1958); *Sov. Phys. JETP* **8**, 70 (1958).
- [11] L. P. Pitaevskii, *ZhETF*, **37**, 1794 (1959); *Sov. Phys. JETP* **10**, 1267 (1960).
- [12] A. A. Abrikosov, L. P. Gor'kov, I. E. Dzialoshinski, *Methods of Quantum Field Theory in Statistical Physics* (Pergamon Press, Oxford, 1965).
- [13] V. A. Khodel, J. W. Clark, M. V. Zverev, *Phys. Rev. B* **99**, 184503 (2019).
- [14] A. A. Abrikosov, L. P. Gor'kov, *Sov. Phys. JETP* **12**, 1243 (1960).
- [15] L. P. Gor'kov, *Theory of Superconducting Alloys*, edited by K. H. Bennemann and J. B. Kettelson, *Superconductivity Vol. 1* (Springer-Verlag, New York, 2008).
- [16] A. B. Migdal, *Theory of Finite Fermi Systems and Applications to Atomic Nuclei* (Wiley, New York, 1967).
- [17] V. A. Khodel et al., *JETP Lett.* **92**, 532 (2010).
- [18] V. A. Khodel, J. W. Clark, M. V. Zverev, *Physics of Atomic Nuclei* **74**, 1237 (2011).
- [19] J. A. N. Bruin et al., *Science* **339**, 804 (2013).
- [20] I. M. Halatnikov, *An Introduction to the Theory of Superfluidity* (Benjamin, New York, 1965).